INSTITUTE OF PHYSICS PUBLISHING PHYSICS IN MEDICINE AND BIOLOGY

Phys. Med. Biol. **48** (2003) 2255–2268 PII: S0031-9155(03)60592-0

Ratiometric fluorescence polarization as a cytometric functional parameter: theory and practice

Yitzhak Yishai, Dror Fixler, Meir Cohen-Kashi, Naomi Zurgil and Mordechai Deutsch

The Biophysical Interdisciplinary Jerome Schottenstein Center for the Research and the Technology of the Cellome, Department of Physics, Bar-Ilan University, Ramat-Gan 52900, Israel

E-mail: rtcellom@mail.biu.ac.il

Received 10 March 2003
Published 14 July 2003
Online at stacks.iop.org/PMB/48/2255

Abstract

The use of ratiometric fluorescence polarization (RFP) as a functional parameter in monitoring cellular activation is suggested, based on the physical phenomenon of fluorescence polarization dependency on emission wavelengths in multiple (at least binary) solutions. The theoretical basis of this dependency is thoroughly discussed and examined via simulation. For simulation, aimed to imitate a fluorophore-stained cell, real values of the fluorescence spectrum and polarization of different single fluorophore solutions were used. The simulation as well as the experimentally obtained values of RFP indicated the high sensitivity of this measure. Finally, the RFP parameter was utilized as a cytometric measure in three exemplary cellular bioassays. In the first, the apoptotic effect of oxLDL in a human Jurkat FDA-stained T cell line was monitored by RFP. In the second, the interaction between cell surface membrane receptors of human T lymphocyte cells was monitored by RFP measurements as a complementary means to the fluorescence resonance energy transfer (FRET) technique. In the third bioassay, cellular thiol level of FDA- and CMFDA-labelled Jurkat T cells was monitored via RFP.

1. Introduction

Fluorescence polarization (FP) is considered to be one of the first measures of cellular functionality used (Cercek *et al* 1974, Shapiro 1995). In the course of cell activation, the processes linking early and late intracellular events involve conformational changes of cytosolic enzymes and/or their regulatory proteins, as well as intracellular matrix re-organization (Ben-Ze'ev and Bernadsky 1997, Geiger *et al* 1982). These early structural changes were monitored by measuring the FP of cellular fluorescent probes (Sunray *et al* 1999, Dimitropoulos *et al* 1986, Kaplan *et al* 1997).

Briefly, the degree of the emission polarization is defined as

$$\mathrm{FP} = \frac{(I_{\parallel} - I_{\perp})}{(I_{\parallel} + I_{\perp})}$$

where $I_{\parallel}$ and $I_{\perp}$ are the emitted field components that are parallel and perpendicular to the excitation field, respectively. If fluorescent motionless molecules, randomly distributed in a dilute solution, are excited by polarized light, it can be shown that the degree of their $\mathrm{FP} \equiv \mathrm{FP}_0$ would be 0.5, provided that the directions of absorption and emission dipole moment (the antennas) are parallel.

The relation between FP, FP_0, τ_{F} (fluorescence lifetime) and the viscosity η of a homogeneous hosting media is given by the Perrin equation (Perrin 1929)

$$\frac{1}{\mathrm{FP}} - \frac{1}{3} = \left(\frac{1}{\mathrm{FP}_0} - \frac{1}{3}\right)\left(1 + \frac{RT}{\eta V}\tau_F\right)$$

where V is the molar volume of a spherical probe, R is the gas constant and T is the absolute temperature. The reciprocal of the ratio $RT/\eta V$ is defined as τ_{R}, the rotational correlation time of the probe. The latter is the most dominant and variable reflecting environmental changes such as temperature, viscosity, mobility and probe binding as monitored by FP. The more limited the rotational motion of the fluorescent probe, the higher the correlation between the excitation and emission polarization, namely the FP, and vice versa. The intracellular environmental influence upon the hosted fluorescent probe is evident.

When monitoring cell functionality, cytometrists more frequently utilize fluorescence intensity (FI) measurements, rather than fluorescence polarization. Nevertheless, unlike FP measurements which are ratiometric (comprising fluorescence intensity ratios), direct FI measurements are strongly dependent on non-relevant variables (instability of the excitation beam, fluctuation in dye concentration, collecting/gathering power of the optical system, the angle between the direction of excitation and detection, etc). For example, since most cytometers—flow and/or static—utilize polarized illumination, it can be readily shown that the ratio between the measured FI and the real total FI emission is polarization dependent and equals 2/3-P, where P is the emitted FP. Thus, for the same intracellular dye concentration, similar cells which possess different intracellular viscosities, or other environmental characteristics which influence their FP, will yield different misleading FI intensities (Deutsch *et al* 2002). This argument also holds true when the excitation beam (normal to the detection direction) is natural-polarized (unpolarized). Therefore, if accurate FI measurements are desired, the total FI should be calculated out of the vertical and horizontal component of the emission, when polarized excitation is employed. Furthermore, the FP measurement inherently contains information that FI does not. While FI indicates the presence of a fluorophore, FP, due to its strong dependency on the fluorophore mobility restrictions, distinguishes between free and bound/associated probe, and, as a result, between specific (relevant) and non-specific staining. Last but not least, most of the cases where fluorescence resonance energy transfer (FRET) occurs can be elegantly, easily and inexpensively detected by measuring the ratio between the donor and acceptor FP values, namely by the ratiometric fluorescence polarization (RFP). This is due to the fact that FRET accelerates the evacuation of the donor excited state, thus shortens its fluorescence lifetime and, as a result, increases its FP.

Environmental changes usually tend to alter the FP as well as the emission spectra of a hosted fluorophore. This is exactly what makes RFP a sensitive indicator of cellular functionality, as will be shown in the present study.

In a heterogeneous environment, such as cellular media, different zones may possess various physiochemical features, which dissimilarly influence the spectroscopic characteristics of fluorescent molecules hosted in the different zones. As a result, the FP may be emission wavelength dependent, FP(λ_{em}). Such dependence is uncommon for fluorescent homogeneous solutions. Fluorescence emission normally takes place at the lowest excited electronic level, and hence cannot allow variation of the emission dipole direction, which defines FP(λ_{em}), with the emission wavelength, determined by the particular vibronic transition associated with the return of the molecule to its electronic ground state.

The present study introduces a simple mechanism which may explain this dependency and the resulting mathematical formulation which enables both simulation and prediction of various FP(λ_{em}) spectra. Finally, several exemplary uses of RFP as a cytometric functional parameter are presented.

In the following, for brevity, λ stands solely for the *emission* wavelength

2. Theory

The total FP (P_T) of an ensemble of n fluorescent components, measured by a detector at a given emission wavelength, is the intensity weighted summation:

$$P_T = \frac{\sum_{j=1}^{n} I_j^{\parallel} - \sum_{j=1}^{n} I_j^{\perp}}{\sum_{j=1}^{n} I_j^{\parallel} + \sum_{j=1}^{n} I_j^{\perp}} = \frac{\sum_{j=1}^{n} (I^{\parallel} - I^{\perp})_j}{\sum_{j=1}^{n} (I^{\parallel} + I^{\perp})_j}$$

$$= \frac{\sum_{j=1}^{n} (I^{\parallel} - I^{\perp})_j \cdot [(I^{\parallel} + I^{\perp})/(I^{\parallel} + I^{\perp})]_j}{I_T} = \frac{\sum_{j=1}^{n} P_j I_j}{I_T} \tag{1}$$

where P_j and $I_j = (I_{\parallel} + I_{\perp})_j$ (the summation of the parallel and normal polarized fluorescence intensity components in relation to the excitation electric field vector) are, respectively, the local measured FP and fluorescence intensity (FI) of j zone, and I_T is the ensemble's total FI measured by the detector.

For brevity, let us consider a *model consisting of two media (a and b), each possessing different physiochemical properties, which differently influence the spectroscopic characteristics of the hosted fluorophores*. The resulting total emitted fluorescence intensity FI(I_T) and FP(P_T) are then respectively:

$$I_T(\lambda) = \sum I_i(\lambda) = I_a(\lambda) + I_b(\lambda) \tag{2}$$

$$P_T(\lambda) = \frac{\sum I_i(\lambda) P_i}{\sum I_i(\lambda)} = \frac{I_a(\lambda) P_a + I_b(\lambda) P_b}{I_a(\lambda) + I_b(\lambda)}. \tag{3}$$

Rewriting the definitions, and arbitrarily choosing $P_a > P_b$, we obtain for any λ:

$$P_a = \frac{I_a P_a + I_b P_a}{I_a + I_b} > \frac{I_a P_a + I_b P_b}{I_a + I_b} = P_T > \frac{I_a P_b + I_b P_b}{I_a + I_b} = P_b. \tag{4}$$

Or, in short, $P_a > P_T > P_b$. Hence, the total FP of the mixture cannot be smaller than the lowest FP component, or greater than the highest FP component. This is true for any number of different fluorescent molecules, under the supposition that inter-molecular interactions are negligible.

Now, let us examine the nature of $P_T(\lambda)$. In order to find its extremum values, a derivation of equation (3), according to λ, should be performed:

$$\frac{dP_T(\lambda)}{d\lambda} = \frac{[I'_a(\lambda)I_b(\lambda) - I_a(\lambda)I'_b(\lambda)]P_a + [I'_b(\lambda)I_a(\lambda) - I_b(\lambda)I'_a(\lambda)]P_b}{[I_a(\lambda) + I_b(\lambda)]^2}.$$

Since the denominator of $\frac{dP_T(\lambda)}{d\lambda}$ does not determine its sign, we shall concentrate solely on the numerator derivation. Following simple mathematical manipulations, one finds that the numerator equals:

$$[I'_a(\lambda)I_b(\lambda) - I_a(\lambda)I'_b(\lambda)](P_a - P_b) = \frac{d}{d\lambda}\left[\frac{I_a(\lambda)}{I_b(\lambda)}\right] I^2{}_b(\lambda)[P_a - P_b]. \tag{5}$$

The right part of the equation indicates:

(i) When $P_a \neq P_b$, say $P_a > P_b$, then the derivative of $P_T(\lambda)$ is proportional to the derivative of the fluorescence intensity ratio (FIR) $I_a(\lambda)/I_b(\lambda)$, namely $\frac{d}{d\lambda}P_T(\lambda)\alpha\frac{d}{d\lambda}\left[\frac{I_a(\lambda)}{I_b(\lambda)}\right]$. Thus, whenever the derivative of FIR(λ) changes sign, both FIR and P_T have an extremum point at the same wavelength.

(ii) A change in the relative dye concentration will only change the FIR by a constant factor and hence will not affect the locations of the extremum points of FIR(λ), $P_T(\lambda)$ or their behaviour.

(iii) When $P_a = P_b$, then $dP_T(\lambda)/d\lambda = 0$ and $P_T(\lambda)$ is constant.

(iv) Since FP and fluorescence anisotropy (FA) correlate, it can be easily shown that the above holds true for FA as well.

3. Materials and methods

3.1. Fluorescent solutions

Five homogeneous glycerine fluorescent solutions were prepared in degassed glycerine–water mixture: 5 μM Fluorescein (Sigma, St Louis, MO, USA), in 30% and 60% glycerine in water, pH = 7.4, 5 μM LysoSensor Blue (Molecular Probes Eugene, OR, USA), pH = 5 in 20% glycerine in water, and two solutions of Carboxy SNARF-1 (Molecular Probes Eugene, OR, USA), pH = 6 and pH = 9, dissolved in 60% and 30% glycerine in water, respectively. Following the mixing, the solutions were incubated overnight at 37 °C in order to ensure homogeneous and isotropic Perrin solution.

3.2. Simulations of FP(λ)

The measured FI(λ) and FP of fluorescein, LysoSensor Blue and Carboxy SNARF-1 were used for the simulation of FP(λ). In the case of the first two, relative concentration change and red shift were, respectively, mathematically mimicked. The simulated $FP_T(\lambda)$ of the binary mimicked solutions (λ) was calculated via equation (3), introducing the measured FP and FI(λ) values. The calculation of FP(λ) from the measured $I_\parallel(\lambda)$ and $I_\perp(\lambda)$ was carried out using the relationship:

$$P(\lambda) = [I_\parallel(\lambda) - G(\lambda)\, I_\perp(\lambda)]/[I_\parallel(\lambda) + G(\lambda)\, I_\perp(\lambda)] \tag{6}$$

where G is the correction factor of the emission monochromator grating. For all calculations, MATLAB software was used.

3.3. Cells

HPBL separation, growth and harvest of a Jurkat T human leukemic cell line were performed, following Zurgil *et al* (1999a).

3.4. Labelling and preparation of cells

The staining procedure of HPBL and the Jurkat cell line with fluorescein diacetate (FDA) and 5-chloromethylfluorescein diacetate (CMFDA) (Zurgil *et al* 1999a), lipoprotein isolation, modification and characterization were performed as described elsewhere (Zurgil *et al* 1999b).

For the induction of apoptosis, cells were incubated in incomplete RPMI 1640 medium in the presence of 0.2–200 μg ml^{-1} oxLDL at 37 °C for 1 h.

For the measurement of cellular surface receptor interaction via RFP, fluorescein conjugated ConA (ConA-F) and tetramethylrhodamine conjugated ConA (ConA-R), both purchased from Vector (Burlingein, CA, USA), were reacted simultaneously with HPBL at the total concentration of 2 μg ml^{-1} at 4 °C for 1 h, yielding double staining. The control samples were cell-labelled with ConA-F plus the equivalent amount of unlabelled ConA in place of ConA-R. The cells were washed once to free them from ConA by centrifugation for 5 min at 4 °C in 5 ml of 5% fetal calf serum (FCS) in PBS.

The induction of capping was carried out following Chahn and Alderete (1990). Briefly, the stained cells were resuspended in 200 μl of RPMI-C (which stands for RPMI 1640 supplemented with 10% heat-inactivated, twice-filtered FCS, 2 mM L-glutamine, 10 mM Hepes, 10 units/ml penicillin and 1× non-essential amino acids), followed by incubation at 37 °C for 1 h. After washing twice and pelting in cold PBS-FBS with 0.1% sodium azide (NaN_3), samples were fixed in 4% formaldehyde. For non-capping conditions, samples were stained at 4 °C in the presence of 0.1% NaN_3 and fixed immediately.

For cellular thiol level estimation via RFP measurements, an aliquot of 50 μl of cell suspension was added to 50 μl of staining solution consisting of various concentrations of FDA or CMFDA in modified PBS, and incubated either at room temperature for 5 min, or at 37 °C for 30 min.

3.5. Instrumentation

Measurements of the solutions' FI and FP were performed by Aminco-Bowman Series 2, SLM (Aminco Spectronic Instruments, New York, USA) spectrofluorimeters. The excitation wavelengths were 488 nm for fluorescein, rhodamine and Carboxy SNARF-1, and 340 nm for LysoSensor Blue. In all the measurements, the width of the emission and excitation slits was 2 nm.

For the cytometric measurement, the FI of stained cells was measured by our in-house designed individual cell scanner (ICS). Briefly, the ICS is a multi-parametric computerized discrete cytometer. Its central feature is a cell tray incorporating an array of individual cell receptacles. Figure 1 shows a two-dimensional array of stained cells orderly located in their receptacles on the cell tray. The cell tray is mounted on a computer-controlled stage, which enables repeated multi-scanning of the same cells. In the present study, cells were illuminated with 1–5 μW 442 nm light from a He–Cd laser. Under the staining conditions used here, the time necessary to obtain 10,000 counts of fluorescence from a single stained cell ranged from 1 to 500 ms. The software that we have designed enables the determination of the range and other statistical characteristics of all measured parameters for either the entire cell population or an operator-selected subpopulation before, during or after biological manipulation on the cells.

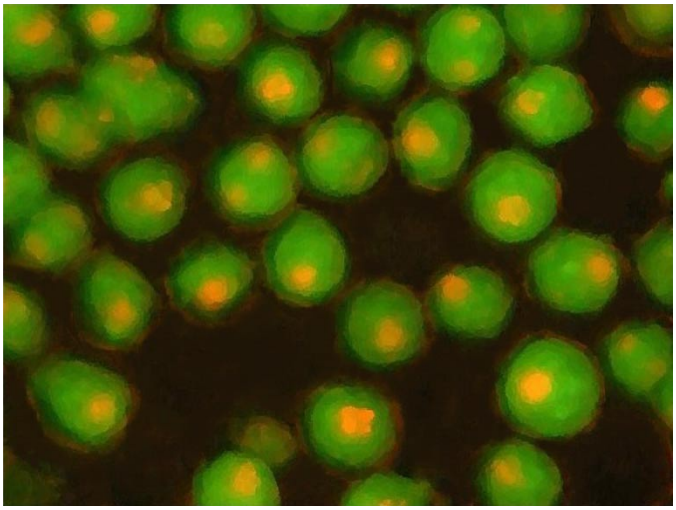

Figure 1. U937 monocytes vitally stained with Acridine orange (5 μM). The cells are orderly and individually settled in the receptacles of the ICS cell tray. The red and green fluorescent regions indicate, respectively, high probe concentration within lysosomes, and low probe concentration in the cytosol.

4. Results

4.1. The measurements and simulation of homogeneous fluorescent solutions' FI(λ) and FP(λ)

Ideally, one would aspire to experimentally mimic a *stained cellular multi-domain structure*. Practically, due to technical difficulties encountered when constructing a miniature measurement multi-sectional chamber, a simulation of FP(λ) of binary homogeneous mixtures was performed using the measured FI and FP spectra of the different solutions.

The measured FI(λ) and FP(λ) emission spectra of 5 μM fluorescein in 30% and 60% glycerine–water are shown in the inset of figure 2. The emission of the latter is red shifted, quenched and narrowed. The FP(λ) are constant and respectively equal 0.125 ± 0.007 and 0.174 ± 0.01.

Utilizing these data, the binary mixture FP(λ) was simulated according to equation (3) (figure 2). Indeed, the simulated FP(λ) indicates a 'peak-like' behaviour (graph I), which follows FIR(λ) (data not shown). Moreover, simulating a change in the relative dye concentration (multiplying graph 'a' in the inset by 3) alters the mixture's FP(λ) by a constant factor but does not affect its behaviour (graph II).

In order to mimic situations in which the same dye is hosted by a medium which is heterogeneous with respect to pH and viscosity, the visible light-excitable fluorescent pH indicator Carboxy SNARF-1 (Whitaker *et al* 1991) was used. The FI(λ) of two Carboxy SNARF-1 solutions, having pH = 6 and 9 (graphs I and II, figure 3) and constant FP values of, respectively, 0.3 and 0.12 (data not shown), were measured. The results indicate that elevation of pH shifts the fluorescence towards red and alters its shape. The simulated FP(λ) of the binary mixture of Carboxy SNARF-1, calculated from the actual data (graphs I and II), yielded a bell-shaped dependency (graph III). In case of a mixture of dyes having complex emission spectrum, the theory predicts a multi-peak FP(λ) dependency. In the present study,

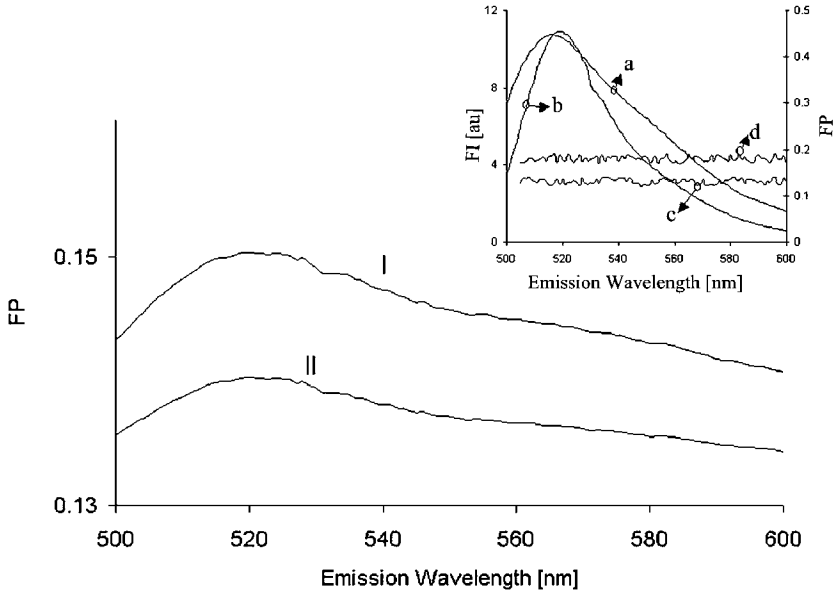

Figure 2. Simulation of FP(λ) of a binary mixture: I—utilizing the actual measured data of FI(λ) and FP, shown in the inset, and II— as in I, except that FI(λ), marked 'a' in the inset, was multiplied (intensified) by a factor of 3. In the inset: emission spectra of 5 μM fluorescein in glycerine water solutions, 30% -a, 60%-b and their corresponding FP(λ): 0.125 ± 0.007 (graph c) and 0.174 ± 0.01 (graph d). Measurements were performed at room temperature on spectrofluorimeters Aminco-Bowman Series 2 and SLM. The excitation wavelength was 488 ± 2 nm.

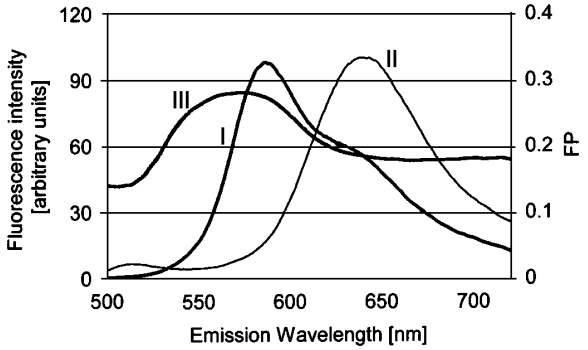

Figure 3. Simulation of the FP of a binary mixture of Carboxy SNARF-1. Real data graphs, I (pH = 6, FP = 0.3) and II (pH = 9, FP = 0.12), were used for the simulation of FP(λ) shown in graph III. Measurements were performed at room temperature on Aminco-Bowman Series 2 spectrofluorimeter. Excitation wavelength: 488 ± 2 nm.

this phenomenon was simulated via LysoSensor Blue which was previously used for ratio imaging of pH in acidic organelles such as lysosomes (Diwu *et al* 1999).

The FP of 5 μM LysoSensor Blue dissolved in 20% glycerine in water (pH = 5) is 0.11 ± 0.01. Its fluorescence spectrum is depicted in figure 4 (graph a), and exhibits dual-emission spectral peaks. For the simulation of FP(λ) of a binary mixture, the LysoSensor Blue spectrum was mimicked by mathematical 3 nm red shifting of graph a, yielding graph b to

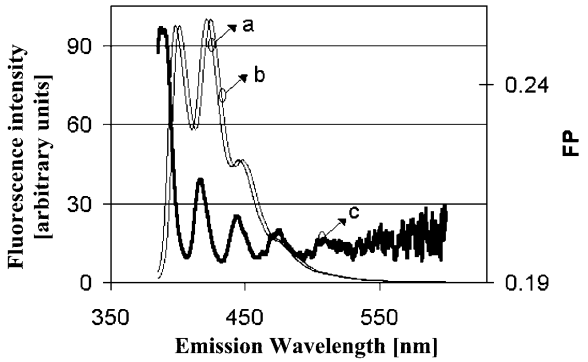

Figure 4. Simulated FP(λ) of a binary mixture of LysoSensor Blue. The real emission spectrum of LysoSensor Blue (graph a), and its FP = 0.11 were measured at room temperature by the Aminco-Bowman Series 2 spectrofluorimeter. Excitation wavelength: 340 ± 2 nm. Graph b represents a 3 nm mathematically red shifted image of graph a to which FP of 0.22 was attributed. Graph c represents the simulated FP(λ) of a binary mixture of LysoSensor Blue, which was obtained by combining graphs a and b via equation (3).

which a constant FP value of 0.22 is related. The simulated mixture FP(λ) yielded a strong wavelength dependent decayed and wavy function (graph c).

4.2. RFP measurement of fluorescent probe labelled cells

4.2.1. Monitoring apoptotic effects of oxLDL in human Jurkat T cell line. One of the earliest events in atherosclerosis, a lethal disease characterized by lesions in blood vessels, is the initial accumulation of oxidized low-density lipoprotein (ox-LDL) that is considered a principal factor in the development of the disease. Ox-LDL has a powerful cytotoxic effect; it causes necrosis and/or apoptosis of different types of cells including T-lymphocytes. Since cell death could contribute to the lesion development and stability, the detection of the apoptotic process at an early stage is of great importance. We had previously shown that fluorescein fluorescence hyperpolarization which accompanied cell dehydration is an early measure of apoptosis (Zurgil *et al* 2000). Here we utilized the RFP measurements to monitor early apoptotic events induced by ox-LDL in a human Jurkat T cell line, a model of T cell response in atherogenic plaques.

Figure 5 shows the dose response curve of the RFP change in oxLDL-treated Jurkat T cells, measured 60 min following the induction of apoptosis. The mean RFP of the FDA labelled cell population, measured at 530 and 510 nm, was 1.12. A decrease in RFP values is evident upon incubation of the cells in the presence of ox-LDL at concentrations as low as 2 μg ml^{-1}, reaching a maximum decrease of 10% at the oxLDL concentration of 20 μg ml^{-1}.

No change could be detected in the same cell population following 1h of oxLDL exposure with respect to other early apoptotic parameters: neither in the PS externalization, nor in mitochondrial membrane potential as measured by AnnexineV and Rhodamine 123, respectively.

4.2.2. Monitoring of cell surface receptor interaction via RFP measurements. A wide range of problems arising in molecular biology, particularly those relating to surface receptor interaction and/or proximity, was addressed by the measurement of fluorescence resonance energy transfer (FRET). These measurements were based mostly on the estimation of energy

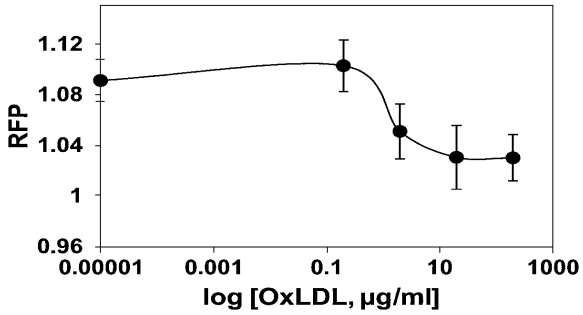

Figure 5. The oxLDL dose response curve of mean RFP values of a Jurkat cell line. The response was measured 1 h following exposure of FDA labelled cells to oxLDL. Values are mean of four different experiments and SD. Measurements were performed at room temperature, utilizing the ICS. Individual cells were excited with He–Cd laser, 4 μW per cell at 442 nm, their FP was measured at the emission wavelengths of 530 and 510 nm. At ox-LDL concentrations smaller than 0.1 μg ml^{-1}, the mean cell population RFP value is about 1.12 and then steeply drops to about unity towards oxLDL concentration of 20 μg ml^{-1}. This decline in RFP values was found to precede the well-established early apoptotic indicators: the PS externalization and changes in the mitochondrial membrane potential.

transfer efficiency (E) via measurements of donor fluorescence lifetime and the relative changes in donor/acceptor emission intensities (Stryer 1978, Epe *et al* 1982, Damjanovich *et al* 1977). In the following example, RFP is suggested as an additional and 'easy to perform' tool for monitoring the extent of surface receptor interaction. The physical rationale behind this approach is that when the proximity (few tens of angstroms or less) between the donor and acceptor fluorescent molecules allows energy to be transferred from the former to the latter (via non-radiative dipole-dipole interaction), an additional path for evacuation of the donor excited level becomes available. As a result, the donor's fluorescent lifetime decreases and, consequently, its FP increases. This effect may be emission wavelength dependent when FP is measured in two wavelengths, where one represents primarily the donor emission and the other represents the acceptor emission. This idea was examined by utilizing model experiments in human T lymphocyte cells. Patching and capping were induced via ConA. Capping is a physical phenomenon occurring in lymphocyte membranes in which surface protein macromolecules become oriented and form a dense cluster at one pole of the cell (Chahn and Alderete 1990). It was, therefore, expected that the RFP values of capping induced cells [c] would be greater than those obtained from cells with no capping induced [nc].

Utilizing the ICS, individual cell RFP = FP(530 nm)/FP(580 nm) measurements were performed. Four groups of variously treated cells were measured for their RFP: capping induced cells [c] and cells with no capping induced [nc], each labelled with ConA-F alone (F[c] and F[nc] respectively) and both with ConA-F and ConA-R (FR[c] and FR[nc], respectively). In each experiment, about 400 cells were measured and their average RFP calculated.

The experiments were carried out in triplicate. The mean RFP values of the three different experiments, and their average deviations from that mean, are listed in table 1.

4.2.3. Monitoring of cellular thiol via RFP. Cellular thiol levels regulate lymphocyte proliferation and death, and play a significant role in the immune response. Therefore, the ability to analyse the total protein and non-protein thiol compounds and their distribution among individual living lymphocytes is of great importance. The discernable effect of bound fluorophore molecules having a higher FP and shifted emission spectrum relative to free ones,

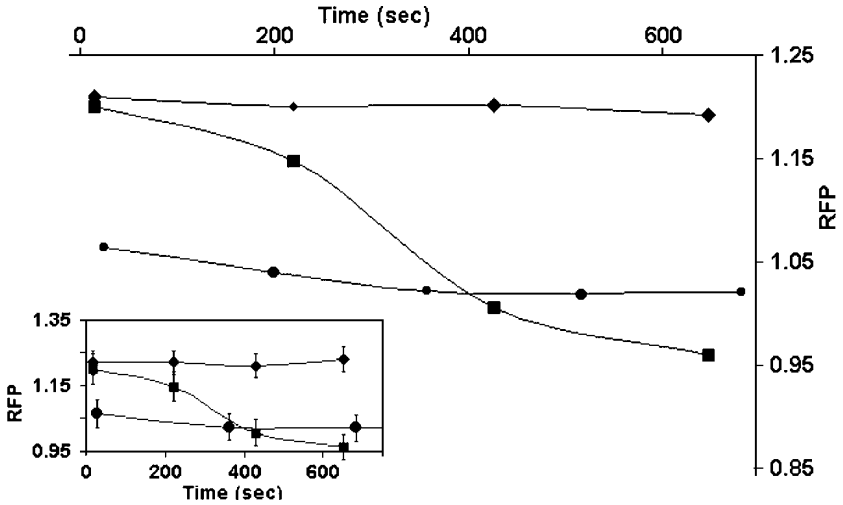

Figure 6. The time dependence of RFP of three individual representative Jurkat T cells, and of cell population (the inset), labelled with 1.2 μM FDA (♦), and CMFDA at concentrations of 10 μM (■) and 5 μM (●). In the inset, the data concerning CMFDA-stained cells were taken from Zurgil *et al* (1999a). Measurements were performed by the ICS, 30 min following staining to ensure a complete conversion of CMFDA to SH-F, for 700 s at room temperature. Individual cells were excited with He–Cd laser, 4 μW per cell at 442 nm, while their FP was measured at the emission wavelengths of 530 and 510 nm.

Table 1. FP and RFP values of surface stained cells.

Experiment	P_1 (530 nm)	P_2 (580 nm)	RFP $= P_1/P_2$
F[nc]	0.227 ± 0.003	0.279 ± 0.003	0.813 ± 0.017
F[c]	0.223 ± 0.002	0.277 ± 0.001	0.805 ± 0.010
FR[nc]	0.233 ± 0.002	0.236 ± 0.004	0.987 ± 0.027
FR[c]	0.250 ± 0.002	0.165 ± 0.001	1.515 ± 0.023

Monitoring of capping via RFP in HPBL. Fluorescein and fluorescein-rhodamine labelled cells are respectively marked by F and FR, and [c] and [nc] stand for capping and no capping, respectivley.

was used in order to estimate the proportional fractions of thiol bound fluorophores in living lymphocytes.

In the present experiment, the cellular thiol levels were monitored by RFP, utilizing CMFDA. CMFDA is a non-fluorescent membrane-permeable probe that is intracellularly hydrolyzed to fluorescent 5-chloromethyl flourescein (CMF). The latter reacts with thiols to form an impermeant, bound fluorescent aldehyde-conjugate product (SH-F), but may stay partially unbound (Hedley and Chow 1994) while possessing spectroscopic properties similar to those of FDA hydrolyzed to unbound cellular fluorescein.

The RFP(t) of FDA- and CMFDA-labelled Jurkat T cells (three individual representative cells randomly chosen), measured at 530 and 510 nm for 700 s, is shown in figure 6. The measurements were performed 30 min after the staining in order to assure the complete conversion of CMFDA to SH-F.

At short times after the measurements' onset, the RFP values in Jurkat T cells, labelled with 1.2 μM FDA (♦) (which was used as control of the unconjugated fluorophore) and

10 μM CMFDA (■), are higher than 1.15. While the RFP of the former is quite constant, that of the latter gradually decreases to a final value nearing unity.

The RFP of the unconjugated fluorophore (FDA labelled cells) may indicate that the RFP of approximately 1 represents the thiol bound molecules (SH-F), while the RFP of about 1.2 and above represents the intermediate phase of conjugated-unconjugated fluorophores. This may lead to the interpretation that RFP(t) of CMFDA, which varies in time from values higher than 1.2 to approximately 1, may monitor the conversion of the intermediate phase CMF into SH-F adducts.

A more moderate time dependency of RFP is observed for a lower concentration of CMFDA (5 μM, ●), where RFP(t) tends to unity. This result suggests that, for these lower CMFDA concentrations, the bound fluorophore, rather than the unbound, is dominant at all time points. This correlation between CMFDA concentrations and RFP values can be accounted for by a two-stage process, whereby a high yield esterase hydrolysis is followed by a low yield transferase reaction. The results presented in figure 6 suggest that a high CMFDA concentration (10 μM) causes a temporary accumulation of unbound CMF, yielding a high RFP. They are later (after approximately 300 s) processed by the transferase to SH-F, resulting in a lower RFP ($\approx$1). On the other hand, at lower CMFDA concentrations (5 μM), the CMF production rate is equal to or lower than that of the transferase product SH-F. Thus, the accumulation of the free molecules is very slow, causing the production of SH-F to be the dominant process manifested by an RFP value of $\approx$1 at all times. The veracity of the phenomenon discussed above and presented in only three representative cells (figure 6) is supported by its conservation in cell population as well, despite the deviation, as shown in the inset of figure 6.

5. Discussion

The effects of solvents can be dramatic, and a complete change of the spectroscopic nature of a fluorescent solute can occur with a change of solvent. For example, in non-binding solvents, the pH, polarity, polarizability, viscosity, etc can be the determinants of the fluorescence emission red shift. On the other hand, the degree of extensiveness of solute/solvent interaction can determine red shifted emission solely due to solute binding, rather than due to the electrostatic solvent effect. Owing to a higher polarity of most polar aromatic molecules (whose lowest single electronic states are π, π^*) in the excited than in the ground electronic state (Guilbault 1967), they tend to interact with polar solvents as to align the solvent dipoles. In such alignment, the energy of the excited state is reduced causing the red shift of the emission spectra. This occurs even in the case of non-polar solvents and solutes, since excitation by itself induces electrostatic polarization of the hosting medium (Campbell and Dwek 1984). Interestingly enough, in the case of fluorescein, the red shift increases as solvent polarity decreases (Meisingset and Steen 1981). The cellular content has a lower polarity relatively to that of the suspending PBS solution. This can account for the red shift of intracellular fluorescein emission compared to that of fluorescein in disrupted FDA labelled cell solution (data not shown).

The mechanism of the red shift discussed here would be enough to account for the case when a cell, stained with a mono-fluorophore, appears as if stained with an ensemble of 'dissimilar probes'. If these seemingly dissimilar probes experience different levels of viscosity, then an emission wavelength FP dependency for the entire stained cell may be anticipated.

Generally, the case of 'two poles apart' emission of dyes is not interesting. Let us assume $I_a(\lambda)$ is distributed at the short wavelengths, and $I_b(\lambda)$ in the long wavelength region. Hence,

at short wavelengths $I_b \to 0$ and thus FIR $= I_a(\lambda)/I_b(\lambda)$ tends to infinity, while in the long wavelength region, $I_a \to 0$, and FIR tends to zero. Dividing the ratio on the right-hand of equation (2) by I_b one obtains:

$$P_T(\lambda) = \frac{[I_a(\lambda)/I_b(\lambda)]\, P_a + P_b}{[I_a(\lambda)/I_b(\lambda)] + 1} = \begin{vmatrix} P_a; \text{for}[I_a(\lambda)/I_b(\lambda)] \to \infty \\ \\ P_b; \text{for}[I_a(\lambda)/I_b(\lambda)] \to 0 \end{vmatrix}. \tag{7}$$

This is a step function. In our case, where $P_a > P_b$, one should expect a polarization emission spectrum consisting of a relatively high and constant FP section at the shorter wavelengths, which continuously and moderately decreases towards the longer wavelengths to a low and constant FP section.

The physical aspect of the present study considers solely the additive effect, in which the total measured FP of a mixture of fluorophores is the result of their intensity weighted FP summation. The case of a binary mixture was considered for the sake of brevity. In fact, a stained cell may behave as a multi fluorophore mixture, and consequently may demonstrate a complicated dependency of FP(λ).

Another mechanism that may explain such dependency is the possibility that the emission spectrum of a single fluorophore is composed of different directional vibronic (vibrational-electronic) transitions from the first excited electronic state to the ground state, due to intrinsic intra-molecular bonding distortions. Generally, it is assumed that the electronic transition does not depend on the vibrational transition (the Born–Oppenheimer approximation). However, the binding of marker molecules to a macromolecule may destroy the symmetry restrictions of the electronic transition, so that various vibrational transitions (hence different emission wavelengths) will be affected differently by the bonding forces. It is then possible that certain vibrational transitions will be enhanced, depending on the site of binding, which will also influence the rotational freedom of the fluorescent molecule at the site, thus yielding a relation between the emitted wavelength and the degree of the polarization of emitted radiation.

A proper solution to this problem has not yet been found. It seems, however, that a sensible theoretical solution might require abandoning the Born–Oppenheimer approximation, while considering the implications of the binding of the marker molecule to the macromolecules of the cell and the influence of such binding on the electronic transitions via the vibrational system of the marker.

As for the cytometric measurements, the RFP parameter was sensitive enough to monitor intracellular alterations induced at a low (2 μg ml^{-1}) oxLDL concentration, prior to the manifestation of other morphological or molecular cell death characteristics, as detected in cell populations or single cells by FI measurements performed in flow, static or bulk cytometery.

Concerning the monitoring of cell surface receptor interaction, the results shown in table 1 (part of an extensive study, data not published yet, article in preparation) suggest that RFP can be a handy, easy to use tool for monitoring membrane structural alteration.

Moreover, for a double stained capping induced cell, RFP = 1.515. This result should be compared to the RFP value of its control measurement, namely RFP = 0.805 obtained for F[c] (2nd row of table 1). This comparison indicates an increase of about 90% in RFP value due to capping, a number which is far greater, and thus probably more sensitive than the calculated energy transfer yield (E) that in the present experiment barely reaches 20%. These findings may recommend RFP as an additional measure to FRET for monitoring membrane events.

Finally, we suggest that RFP may discriminate *in situ* between unconjugated CMF and GSH adducts, thus addressing a problem routinely encountered when utilizing FI measurements, namely the high fluorescence background level originating from the unbound CMF molecule, which interferes with the FI measurement of the thiol bound adduct.

6. Conclusion

The present study suggested the ratiometric fluorescence polarization measure as a sensitive and powerful tool for the understanding of molecular interactions. The fact that RFP depends both on the emission spectrum and on the fluorescence polarization of a given fluorophore, makes it a sensitive prospective cytometric tool since the hosting cellular medium is heterogeneous and differently influences the spectroscopic characteristics of the hosted fluorophore. Moreover, when one or several fluorophores specifically localized within the cell are used, RFP becomes a localization specific measure. Measuring RFP is handy, very easy to perform and significantly cheaper than existing assays which aim to achieve, for example, accurate enough FRET measurements, as well as the discrimination between bound (relevant) and free (non-relevant) markers.

Acknowledgment

We would like to thank Ina Solodiev for her contribution to the study of oxLDL induced apoptosis.

References

Ben-Ze'ev A and Bershadsky A D 1997 The role of the cytoskeleton in adhesion-mediated signaling and gene expression *Adv. Mol. Cell. Biol.* **24** 125–63

Campbell I D and Dwek R A 1984 *Biological Spectroscopy* (Menlo Park, CA: Benjamin-Cummings) pp 103–07

Cercek L, Cercek B and Franklin C I V 1974 Biophysical differentiation between lymphocytes from healthy donors, patients with malignant disease and other disorders *Br. J. Cancer* **29** 345–52

Chahn T C and Alderete B E 1990 A rapid method for quantitating lymphocyte receptor capping: capping defect in AIDS patients *J. Viorogical Methods* **29** 257–66

Damjanovich S, Bahr W and Jovin T M 1977 The functional and fluorescence properties of Escherichia coli polymerase reacted with fluorescamin *Eur. J. Biochem.* **72** 559–69

Deutsch M, Tirosh R, Kaufman M, Zurgil N and Weinreb A 2002 Fluorescence polarization as a functional parameter in monitoring living cells: theory and practice *J. Fluorescence* **12** 25–44

Dimitropoulos K, Rolland J M and Nairn R C 1986 Flow cytofluorimetry of fluorescein fluorescence polarization to assay lymphocyte activation *Biochem. Biophys. Res. Commun.* **136** 1021–29

Diwu Z, Chen C S, Zhang C, Klaubert D H and Haugland R P 1999 A novel acidotropic pH indicator and its potential application in labeling acidic organelles of live cells *Chem. Biol.* **6** 411–8

Epe B, Wooley P, Steinhauser K G and Littlechild J 1982 Distance measurement by energy transfer; the 3' end of 16-SRNA and proteins S4 and S17 of the ribosome of Escherichia coli *Eur. J. Biochem.* **129** 211–9

Geiger B, Rosen D and Berke G 1982 Spatial relationships of MTOC and the contact area of cytotoxic T lymphocytes *J. Cell. Biol.* **95** 137–43

Guilbault G G 1967 *Fluorescence: Theory, Instrumentation and Practice* (New York: Marcel Dekker) p 77

Hedley D W and Chow S 1994 Evaluation of methods for measuring cellular glutathione content using flow cytometry *Cytometry* **15** 349

Kaplan M, Trebnyikov E and Berke G 1997 Fluorescence depolarization as an early measure of T Lymphocyte stimulation *J. Immunol. Methods* **201** 15–24

Meisingset K K and Steen H B 1981 Intracellular binding of fluorescein in lymphocytes *Cytometry* **1** 272–8

Perrin F 1929 La fluorscence des solutions *Ann. Phys., Paris* **12** 169–275

Shapiro H M 1995 *Practical Flow Cytometry* 3rd edn (New York: Alan R Liss)

Stryer L 1978 Fluorescence energy transfer as a spectrocopic ruler *Annu. Rev. Biochem.* **47** 819–46

Sunray M, Kaufman M, Zurgil N and Deutsch M 1999 The trace and subgrouping of lymphocyte activation by dynamic fluorescence intensity and polarization measurements *Biochem. Biophys. Res. Commun.* **261** 712–9

Whitaker J E, Haugland R P and Prendergast F G 1991 Spectral and photophysical studies of benzo [c] xanthene dyes: dual emission pH sensors *Anal. Biochem.* **194** 330

Zurgil N, Kaufman M, Solodiev I and Deutsch M 1999a Determination of cellular thiol levels in individual viable lymphocytes by means of fluorescence intensity and polarization *J. Immun. Methods* **229** 23–34

Zurgil N, Levy M, Deutsch M, Gilburd B, George J, Haratz D, Kaufman M and Shoenfeld Y 1999b Reactivity of peripheral blood lymphocytes to oxidized low-density lipoprotein: a novel system to estimate atherosclerosis employing the Cellscan *Clin. Cardiol.* **22** 526–32

Zurgil N, Schiffer Z, Shafran Y, Kaufman M and Deutsch M 2000 Fluorescein fluorescence hyperpolarization as an early kinetic measure of the apoptotic process *Biochem. Biophys. Res. Commun.* **268** 155–63